Electric and anomalous magnetic dipole moments of the muon in the MSSM



JHEP06(2009)020

(http://iopscience.iop.org/1126-6708/2009/06/020)

Published by IOP Publishing for SISSA

Received: *May 4, 2009*
Accepted: *May 14, 2009*
Published: *June 5, 2009*

# Electric and anomalous magnetic dipole moments of the muon in the MSSM

**Kingman Cheung,**[a,b,c] **Otto C. W. Kong**[d] **and Jae Sik Lee**[b]

[a] *Department of Physics, National Tsing Hua University, Hsinchu, Taiwan 300, R.O.C.*
[b] *Physics Division, National Center for Theoretical Sciences, Hsinchu, Taiwan 300, R.O.C.*
[c] *Division of Quantum Phases & Devices, Konkuk University, Seoul 143-701, Korea*
[d] *Department of Physics and Center for Mathematics and Theoretical Physics, National Central University, Chung-Li, Taiwan 32054, R.O.C.*
*E-mail:* cheung@phys.nthu.edu.tw, otto@phy.ncu.edu.tw, jslee@phys.cts.nthu.edu.tw

Abstract: We study the electric dipole moment (EDM) and the anomalous magnetic dipole moment (MDM) of the muon in the CP-violating Minimal Supersymmetric extension of the Standard Model (MSSM). We take into account the contributions from the chargino- and neutralino-mediated one-loop graphs and the dominant two-loop Higgs-mediated Barr-Zee diagrams. We improve earlier calculations by incorporating CP-violating Higgs-boson mixing effects and the resummed threshold corrections to the Yukawa couplings of the charged leptons as well as that of the bottom quark. The analytic correlation between the muon EDM and MDM is explicitly presented at one- and two-loop levels and, through several numerical examples, we illustrate its dependence on the source of the dominant contributions. We have implemented the analytic expressions for the muon EDM and MDM in an updated version of the public code `CPsuperH2.0`.

Keywords: Supersymmetry Phenomenology

ArXiv ePrint: 0904.4352



doi:10.1088/1126-6708/2009/06/020

JHEP06(2009)020

## Contents



JHEP06(2009)020

## 1 Introduction

The anomalous magnetic dipole moment of the muon, $a_\mu$, has provided one of the most sensitive test grounds for the validity of the Standard Model (SM) [1]:

$$a_\mu^{\rm EXP} = 11\,659\,208\,(6.3)\ \times 10^{-10}\,. \tag{1.1}$$

At the same time, it also provides an important constraint on new physics with precise SM predictions available. The SM prediction consists of QED, electroweak (EW), and hadronic contributions. The hadronic contribution is further decomposed into leading-order (LO) part and higher-order vacuum polarization (VP) and light-by-light (LBL) parts [2–18]:[1]

$$\begin{aligned} a_\mu^{\rm SM} &= a_\mu^{\rm QED} + a_\mu^{\rm EW} + a_\mu^{\rm Had.(LO)} + a_\mu^{\rm Had.(VP)} + a_\mu^{\rm Had.(LBL)} \\ &= 11\,659\,177.3\,(5.3)\ \times 10^{-10}\,. \end{aligned} \tag{1.2}$$

Equations (1.1) and (1.2) suggest that there is currently a $3.7\,\sigma$ discrepancy between the experimental result and the SM prediction, which can be attributed to possible contributions from physics beyond the SM:[2]

$$\Delta a_\mu^{\rm EXP} \equiv a_\mu^{\rm EXP} - a_\mu^{\rm SM} = 30.7\,(8.2) \times 10^{-10}\ (3.7\,\sigma)\,. \tag{1.3}$$

[1] See table 1 for details of the SM prediction.

[2] The number incorporates the hadronic VP result calculated based on measurements at electron-position storage ring. Calculation based on hadronic $\tau$-decays gives a different result, which is considered less reliable. If the $\tau$-based result is used, the overall discrepancy reduces to only about $1\sigma$.

| | $a_\mu \times 10^{10}$ | $\delta a_\mu \times 10^{10}$ | Ref. |
|---|---|---|---|
| $a_\mu^{\rm QED}$ | 11 658 471.810 | (0.016) | [3–5] |
| $a_\mu^{\rm EW}$ | 15.4 | (0.2) | [6] |
| $a_\mu^{\rm Had.(LO)}$ | 690.9 | (4.4) | [7] |
| $a_\mu^{\rm Had.(LO)}$ | 689.4 | (4.6) | [8] (∗) |
| $a_\mu^{\rm Had.(LO)}$ | 692.1 | (5.6) | [9] |
| $a_\mu^{\rm Had.(LO)}$ | 694.4 | (4.9) | [10] |
| $a_\mu^{\rm Had.(LO)}$ | 691.04 | (5.29) | [11] |
| $a_\mu^{\rm Had.(VP)}$ | −9.8 | (0.1) | [8, 12] |
| $a_\mu^{\rm Had.(LBL)}$ | 8.0 | (4.0) | [13] |
| $a_\mu^{\rm Had.(LBL)}$ | 13.6 | (2.5) | [14] |
| $a_\mu^{\rm Had.(LBL)}$ | 11.0 | (4.0) | [15] |
| $a_\mu^{\rm Had.(LBL)}$ | 11.6 | (4.0) | [16] |
| $a_\mu^{\rm Had.(LBL)}$ | 10.5 | (2.6) | [17] (∗) |
| $a_\mu^{\rm Had.(LBL)}$ | 10.2 | (∼3) | [18] |

**Table 1**. The SM prediction of $a_\mu^{\rm SM}$: see, for example, ref. [2]. For the quoted value in eq. (1.2) we use the results in [8] and [17] for the hadronic leading-order and the hadronic light-by-light contributions, respectively.

One of the most appealing scenarios for physics beyond the SM is augmented with a softly broken supersymmetry (SUSY) around the TeV scale. The supersymmetric contributions to $a_\mu$ from such models are known up to dominant two-loop contributions. The one-loop results can be found in [19–24] and the two-loop results in [25–30]. It is well-known that the dominant two-loop contribution comes from Higgs-mediated Barr-Zee diagrams [31]. The error associated with the known SUSY contributions is estimated to be $\sim 2.5 \times 10^{-10}$ [32], which is smaller than half of the current experimental and SM theoretical ones. On the other hand, the SUSY augmented models can contain additional CP-violating phases beyond the SM Cabibbo-Kobayashi-Maskawa (CKM) phase leading to sizable EDMs [33–36]. The current limit on the muon EDM [37] is

$$|d_\mu| < 1.8 \times 10^{-19}\ \text{e cm}\ (95\%\ \text{C.L.})\,, \tag{1.4}$$

which is much weaker than the constraints from the non-observation of the Thallium [38], neutron [39], and Mercury [40] EDMs:

$$\begin{aligned} |d_{\rm Tl}| &< 9 \times 10^{-25}\ e\,\text{cm}\,, \\ |d_{\rm n}| &< 3 \times 10^{-26}\ e\,\text{cm}\,, \\ |d_{\rm Hg}| &< 2 \times 10^{-28}\ e\,\text{cm}\,. \end{aligned} \tag{1.5}$$



JHEP06(2009)020

Nevertheless, if the muon EDM experiment in the future can achieve the projected sensitivity [41]

$$d_\mu \sim 1 \times 10^{-24}\ e\,\mathrm{cm}\,, \tag{1.6}$$

the precision of the experiment will be comparable to that of the current Thallium EDM experiment.

In this paper, we study the correlation between the muon EDM and MDM in the CP-violating MSSM [30, 42]. We present the relation between the one-loop chargino- and neutralino-mediated EDM and MDM of the muon. We also derive an analytic relation between them in the two-loop contributions from the dominant Higgs-mediated Barr-Zee diagrams. We improve the earlier results by including CP-violating Higgs-boson mixing effects in the Barr-Zee diagrams and resumming the threshold corrections to the muon, tau, and bottom-quark Yukawa couplings in the one- and two-loop graphs. We then focus our numerical studies on three types of scenarios in which (*i*) the muon EDM and MDM are dominated by the one-loop contributions, (*ii*) the lightest Higgs boson is mostly CP odd and lighter than $\sim 50\,\mathrm{GeV}$, and (*iii*) the dominant contributions to the muon EDM and MDM come from the two-loop Barr-Zee graphs.

For the presentation of our analytic results, we follow the conventions and notations of `CPsuperH` [43], especially for the masses and mixing matrices of the neutral Higgs bosons and SUSY particles. The layout of the paper is as follows. Section 2 presents formulas relevant to the one-loop contributions to the muon EDM and MDM from chargino- and neutralino-mediated diagrams. Non-holomorphic threshold effects on the muon Yukawa coupling have been appropriately resummed. In section 3, we present analytic results for the Higgs-mediated two-loop Barr-Zee diagrams. For this, most importantly, the resummed threshold corrections to the tau and bottom-quark Yukawa couplings and the CP-violating Higgs-boson mixing effects have been incorporated. In section 4, we present some numerical examples, depending on the source of dominant contributions to the muon EDM and MDM. We summarize our findings in section 5.

## 2 One-Loop EDMs and MDMs of charged leptons

The relevant interaction Lagrangian of the spin-1/2 lepton with EDM $d_l$ and MDM $a_l$ is given by

$$\mathcal{L}_{\mathrm{spin}-1/2} = -\frac{i}{2}\, d_l\, (\bar{l}\,\sigma_{\mu\nu}\,\gamma_5\, l)\, F^{\mu\nu} + \frac{e\, a_l}{4\, m_l}\, (\bar{l}\,\sigma_{\mu\nu}\, l)\, F^{\mu\nu}\,, \tag{2.1}$$

where $\sigma^{\mu\nu} = \frac{i}{2}[\gamma^\mu\,,\gamma^\nu] = i(\gamma^\mu\gamma^\nu - g^{\mu\nu})$. The EDM and MDM amplitudes are given by

$$(\mathcal{M}_{\mathrm{MDM}})^\mu = \frac{e\, a_l}{2m_l}\, \bar{u}(p')(i\sigma^{\mu\nu}q_\nu)u(p)\,, \qquad (\mathcal{M}_{\mathrm{EDM}})^\mu = d_l\, \bar{u}(p')(\sigma^{\mu\nu}\gamma_5 q_\nu)u(p)\,. \tag{2.2}$$

Generic interactions of charginos $\tilde{\chi}^\pm_{1,2}$ or neutralinos $\tilde{\chi}^0_{1,2,3,4}$, collectively denoted by $\chi$, with a lepton $l$ and a slepton (sneutrino) $\tilde{l}'_{1,2}$ ($\tilde{\nu}_l$) are given by

$$\mathcal{L}_{\chi l\tilde{l}'} = g^{\chi l\tilde{l}'}_{L\,ij}(\bar{\chi}_i P_L l)\, \tilde{l}'^*_i + g^{\chi l\tilde{l}'}_{R\,ij}\, (\bar{\chi}_i P_R l)\, \tilde{l}'^*_j + \mathrm{h.c.} \tag{2.3}$$

The Lagrangian for the interactions of $\chi$ and $\tilde{l}'_{1,2}$ with the photon field $A_\mu$ is

$$\mathcal{L}_{\chi\chi A} = -e\,Q_\chi\,(\bar{\chi}\gamma_\mu\chi)A^\mu \qquad \text{and} \qquad \mathcal{L}_{\tilde{l}'\tilde{l}'A} = -ie\,Q_{\tilde{l}'}\,\tilde{l}'^*\overset{\leftrightarrow}{\partial}_\mu\,\tilde{l}'A^\mu\,. \tag{2.4}$$

The diagrams in figure 1 induce the MDM and EDM of the lepton $l$ as follows:

$$\begin{aligned}(a_l)^\chi &= \frac{m_l^2}{8\pi^2 m^2_{\tilde{l}'_j}}\Bigg\{\left(\left|g^{\chi l\tilde{l}'}_{R\,ij}\right|^2+\left|g^{\chi l\tilde{l}'}_{L\,ij}\right|^2\right)\left[-Q_\chi\,\mathcal{A}(m^2_{\chi_i}/m^2_{\tilde{l}'_j})+Q_{\tilde{l}'}\,\mathcal{B}(m^2_{\chi_i}/m^2_{\tilde{l}'_j})\right]\\ &\qquad +\frac{m_{\chi_i}}{m_l}\,\Re\mathrm{e}\left[\left(g^{\chi l\tilde{l}'}_{R\,ij}\right)^*\,g^{\chi l\tilde{l}'}_{L\,ij}\right]\left[Q_\chi\,A(m^2_{\chi_i}/m^2_{\tilde{l}'_j})+Q_{\tilde{l}'}\,B(m^2_{\chi_i}/m^2_{\tilde{l}'_j})\right]\Bigg\},\\ \left(\frac{d_l}{e}\right)^\chi &= \frac{m_{\chi_i}}{16\pi^2 m^2_{\tilde{l}'_j}}\Im\mathrm{m}\left[\left(g^{\chi l\tilde{l}'}_{R\,ij}\right)^*\,g^{\chi l\tilde{l}'}_{L\,ij}\right]\left[Q_\chi\,A(m^2_{\chi_i}/m^2_{\tilde{l}'_j})+Q_{\tilde{l}'}\,B(m^2_{\chi_i}/m^2_{\tilde{l}'_j})\right],\end{aligned} \tag{2.5}$$

where

$$\begin{aligned}A(r) &= \frac{1}{2(1-r)^2}\left(3-r+\frac{2\ln r}{1-r}\right),\\ B(r) &= \frac{1}{2(1-r)^2}\left(1+r+\frac{2r\ln r}{1-r}\right),\\ \mathcal{A}(r) &= \frac{1}{12(1-r)^3}\left(2+5r-r^2+\frac{6r\ln r}{1-r}\right),\\ \mathcal{B}(r) &= \frac{1}{12(1-r)^3}\left(1-5r-2r^2-\frac{6r^2\ln r}{1-r}\right).\end{aligned} \tag{2.6}$$

We have checked that our analytic expressions for the one-loop MDM and EDM agree with those given in, for example, ref. [23] and [36] with $Q_{\tilde{\chi}_i^-}=Q_{\tilde{l}_j^-}=-1$ and $Q_{\tilde{\chi}_k^0}=Q_{\tilde{\nu}_l}=0$. Note $A(1)=-1/3$, $B(1)=1/6$ and $\mathcal{A}(1)=\mathcal{B}(1)=1/24$. Finally, in eq. (2.5), the chargino-lepton-sneutrino couplings are given by

$$g^{\tilde{\chi}^\pm l\tilde{\nu}}_{L\,i} = -g(C_R)_{i1}\,, \qquad g^{\tilde{\chi}^\pm l\tilde{\nu}}_{R\,i} = h_l^*(C_L)_{i2}\,, \tag{2.7}$$

and the neutralino-lepton-slepton couplings are given by

$$\begin{aligned}g^{\tilde{\chi}^0 l\tilde{l}}_{L\,ij} &= -\sqrt{2}\,g\,T_3^l\,N^*_{i2}\left(U^{\tilde{l}}\right)^*_{1j}-\sqrt{2}\,g\,t_W\,\left(Q_l-T_3^l\right)N^*_{i1}\left(U^{\tilde{l}}\right)^*_{1j}-h_l N^*_{i3}\left(U^{\tilde{l}}\right)^*_{2j},\\ g^{\tilde{\chi}^0 l\tilde{l}}_{R\,ij} &= \sqrt{2}\,g\,t_W\,Q_l\,N_{i1}\left(U^{\tilde{l}}\right)^*_{2j}-h_l^* N_{i3}\left(U^{\tilde{l}}\right)^*_{1j},\end{aligned} \tag{2.8}$$

with $T_3^l=-1/2$ and $Q_l=-1$.

There are non-holomorphic threshold corrections to the Yukawa couplings $h_l$ which appear in the chargino and neutralino couplings [44–46]. These corrections become significant at large $\tan\beta$ and we resum these effects by redefining the Yukawa couplings as follows:

$$h_l = \frac{\sqrt{2}\,m_l}{v\,c_\beta}\,\frac{1}{1+\Delta_l\,t_\beta}\,. \tag{2.9}$$



JHEP06(2009)020

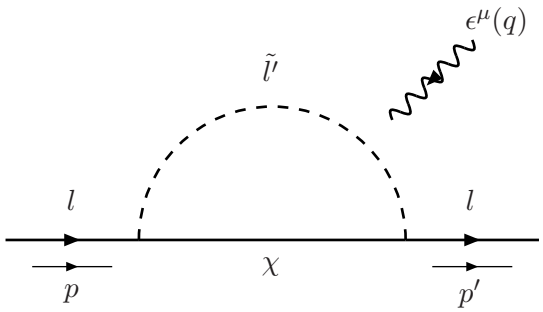


**Figure 1**. Feynman diagrams for the EDM $(d_l)^\chi$ and MDM $(a_l)^\chi$ of the lepton $l$ induced by $\chi$. The photon line can be attached to the slepton $\tilde{l}'$ line or the $\chi$ line.

In the presence of the CP phases, $\Delta_l$ takes the form [47]

$$\begin{aligned}\Delta_l = &-\frac{\alpha_{\rm em}\,\mu^* M_2^*}{4\pi\, s_W^2}\left[ I\left(m^2_{\tilde{\nu}_l}, |M_2|^2, |\mu|^2\right) + \frac{1}{2}\left|U^{\tilde{l}}_{L1}\right|^2 I\left(m^2_{\tilde{l}_1}, |M_2|^2, |\mu|^2\right)\right.\\ &\left. + \frac{1}{2}\left|U^{\tilde{l}}_{L2}\right|^2 I\left(m^2_{\tilde{l}_2}, |M_2|^2, |\mu|^2\right)\right] + \frac{\alpha_{\rm em}\,\mu^* M_1^*}{4\pi\, c_W^2}\left[ I\left(m^2_{\tilde{l}_1}, m^2_{\tilde{l}_2}, |M_1|^2\right)\right.\\ &+ \frac{1}{2}\left|U^{\tilde{l}}_{L1}\right|^2 I\left(m^2_{\tilde{l}_1}, |M_1|^2, |\mu|^2\right) + \frac{1}{2}\left|U^{\tilde{l}}_{L2}\right|^2 I\left(m^2_{\tilde{l}_2}, |M_1|^2, |\mu|^2\right)\\ &\left. - \left|U^{\tilde{l}}_{R1}\right|^2 I\left(m^2_{\tilde{l}_1}, |M_1|^2, |\mu|^2\right) - \left|U^{\tilde{l}}_{R2}\right|^2 I\left(m^2_{\tilde{l}_2}, |M_1|^2, |\mu|^2\right)\right],\end{aligned} \tag{2.10}$$

where the one-loop function is

$$I(x,y,z) \equiv \frac{xy\,\ln(x/y) + yz\,\ln(y/z) + xz\,\ln(z/x)}{(x-y)\,(y-z)\,(x-z)}. \tag{2.11}$$

These effects on the muon MDM have been considered in ref. [29] only in the CP conserving case.

## 3 Barr-Zee graphs

The dominant two-loop contributions come from the Barr-Zee diagrams mediated by neutral Higgs-boson exchanges, see figure 2. Here, we consider loops of third-generation fermions and sfermions, charged Higgs bosons, and charginos. The diagrams can be evaluated first by one-loop computation of the $H_i(k-q)$–$\gamma^\mu(q)$–$\gamma^\nu(k)$ vertex. Thanks to gauge invariance the effective vertex takes the form

$$\Gamma_i^{\mu\nu} = \left[g^{\mu\nu} k\cdot q - k^\mu q^\nu\right]\mathcal{S}_i(k^2) + \left[\epsilon^{\mu\nu\alpha\beta} k_\alpha q_\beta\right]\mathcal{P}_i(k^2), \tag{3.1}$$

where $q$ is the incoming four-momentum of the external photon, $p$ ($p'$) the four-momentum of the incoming (outgoing) lepton, and $k$ the four-momentum of the internal photon going out of the upper loop. Note that $p' = p + q$. Explicitly, keeping only the terms linear in

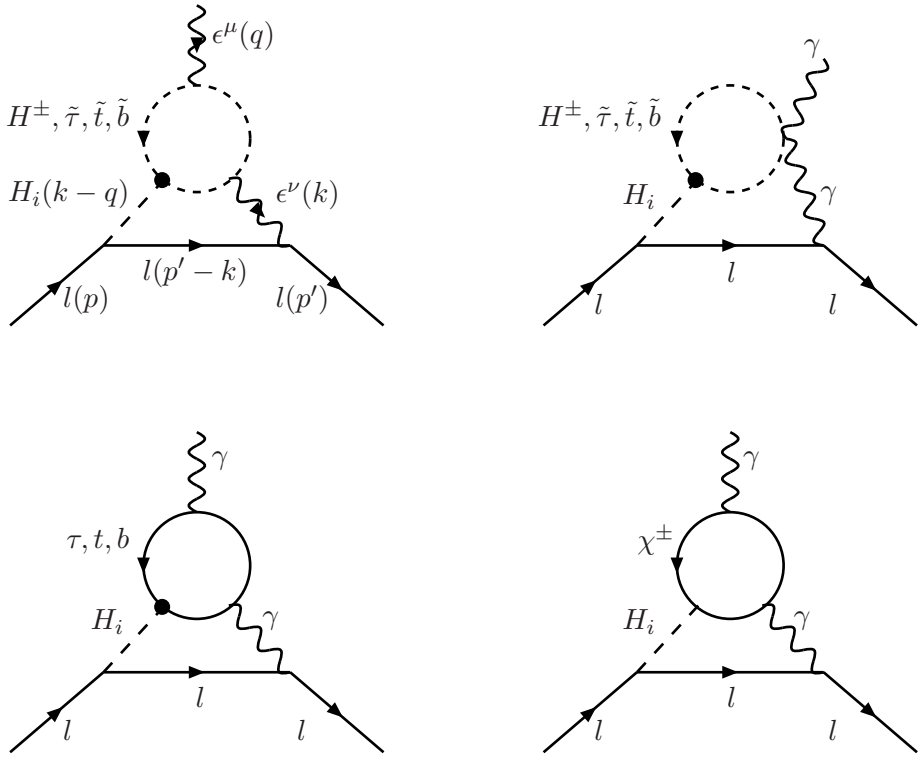


**Figure 2**. Barr-Zee diagrams: the $H_i$ lines denote all three neutral Higgs bosons, including CP-violating Higgs-boson mixing, and heavy dots indicate resummation of threshold corrections to the corresponding Yukawa couplings.

the external momenta, the fermionic contributions are given by

$$\mathcal{S}_i^f(k^2) = -\frac{1}{4\pi^2} N_C^f \, e^2 Q_f^2 g_f m_f \, g^S_{H_i \bar{f} f} \int_0^1 \frac{1-2x(1-x)}{x(1-x)k^2 - m_f^2} \,,$$
$$\mathcal{P}_i^f(k^2) = -\frac{1}{4\pi^2} N_C^f \, e^2 Q_f^2 g_f m_f \, g^P_{H_i \bar{f} f} \int_0^1 \frac{1}{x(1-x)k^2 - m_f^2} \,, \tag{3.2}$$

with the generic $f$-$f$-$H_i$ interaction: $\mathcal{L}_{H_i \bar{f} f} = -g_f \, \bar{f} \, (g^S_{H_i \bar{f} f} + i\gamma_5 \, g^P_{H_i \bar{f} f}) \, f \, H_i$ . The color factor $N_C^f = 3$ for quarks and 1 for leptons and charginos. On the other hand, the sfermion loops contribute only to the scalar form factor as

$$\mathcal{S}_i^{\tilde{f}}(k^2) = \frac{1}{8\pi^2} N_C^f \, e^2 Q_f^2 \, v \, g_{H_i \tilde{f}^* \tilde{f}} \int_0^1 \frac{x(1-x)}{x(1-x)k^2 - m_{\tilde{f}}^2} \,, \tag{3.3}$$

with the generic $\tilde{f}$-$\tilde{f}$-$H_i$ interaction: $\mathcal{L}_{H_i \tilde{f}^* \tilde{f}} = v \, g_{H_i \tilde{f}^* \tilde{f}} \, \tilde{f}^* \tilde{f} \, H_i$ .

Together with the interaction Lagrangian for the couplings of the neutral-Higgs bosons and photon to charged leptons

$$\mathcal{L}_{H_i \bar{l} l} = -g_l \, \bar{l} \, (g^S_{H_i \bar{l} l} + i\gamma_5 \, g^P_{H_i \bar{l} l}) \, l \, H_i \,, \qquad \mathcal{L}_{A \bar{l} l} = -e \, Q_l \, \bar{l} \, \gamma^\mu \, l \, A_\mu \,, \tag{3.4}$$



JHEP06(2009)020

where $g_l = \frac{g\, m_l}{2M_W}$ (as in the `CPsuperH` convention), the Barr-Zee amplitude is given by

$$i\,\mathcal{M}^{\mu}_{\rm Barr-Zee} = \tag{3.5}$$
$$eg_l Q_l \int \frac{\mathrm{d}^4k}{(2\pi)^4} \frac{\bar{u}(p')\left[\Gamma_i^{\mu\nu}\gamma_\nu\,(-\not{k})\,(g^S_{H_i\bar{l}l} + i\gamma_5\, g^P_{H_i\bar{l}l}) + (g^S_{H_i\bar{l}l} + i\gamma_5\, g^P_{H_i\bar{l}l})\,(\not{k})\,\Gamma_i^{\mu\nu}\gamma_\nu\right] u(p)}{k^2\,k^2\,(k^2 - M^2_{H_i})}\,,$$

where again we keep only the terms linear in the external momenta. We note the numerator of the integrand is proportional to

$$\left(g^S_{H_i\bar{l}l}\,\mathcal{S}_i - g^P_{H_i\bar{l}l}\,\mathcal{P}_i\right)(i\sigma^{\mu\nu}q_\nu) - \left(g^P_{H_i\bar{l}l}\,\mathcal{S}_i + g^S_{H_i\bar{l}l}\,\mathcal{P}_i\right)(\sigma^{\mu\nu}\gamma_5 q_\nu)\,. \tag{3.6}$$

We observe that the first term gives the MDM while the second one gives the EDM of the lepton $l$. Consequently, the Barr-Zee contributions to the MDM and EDM are related by

$$(a_l)^H = 2m_l \left(\frac{d_l}{e}\right)^H \Bigg|_{\substack{g^S_{H_i\bar{l}l} \to g^P_{H_i\bar{l}l} \\ g^P_{H_i\bar{l}l} \to -g^S_{H_i\bar{l}l}}}\,, \tag{3.7}$$

with normalizations of the MDM and EDM of the lepton $l$ as given by eq. (2.1). For the dipole moment diagrams with chirality flip inside the loop, the MDM and EDM parts correspond directly to real and imaginary parts of the overall amplitude. The above relation is a recasting of that statement in terms of the effective scalar and pseudoscalar couplings of the generally CP-mixed Higgs states involved. To give the MDM result explicitly, with $Q_l = -1$, we have[3]

$$\begin{aligned}
(a_l)^H = \sum_{q=t,b} \Bigg\{ & -\frac{3\alpha_{\rm em}\,Q_q^2\,m_l^2}{16\pi^3} \sum_{i=1}^{3} \frac{g^S_{H_i l^+ l^-}}{M^2_{H_i}} \sum_{j=1,2} g_{H_i\tilde{q}_j^*\tilde{q}_j}\, F(\tau_{\tilde{q}_j i}) \\
& + \frac{3\alpha_{\rm em}^2\,Q_q^2\,m_l^2}{4\pi^2 s_W^2 M_W^2} \sum_{i=1}^{3} \left[-g^S_{H_i l^+ l^-} g^S_{H_i\bar{q}q}\, f(\tau_{qi}) + g^P_{H_i l^+ l^-} g^P_{H_i\bar{q}q}\, g(\tau_{qi})\right] \Bigg\} \\
& - \frac{\alpha_{\rm em}\,m_l^2}{16\pi^3} \sum_{i=1}^{3} \frac{g^S_{H_i l^+ l^-}}{M^2_{H_i}} \sum_{j=1,2} g_{H_i\tilde{\tau}_j^*\tilde{\tau}_j}\, F(\tau_{\tilde{\tau}_j i}) \\
& + \frac{\alpha_{\rm em}^2\,m_l^2}{4\pi^2 s_W^2 M_W^2} \sum_{i=1}^{3} \left[-g^S_{H_i l^+ l^-} g^S_{H_i\tau^+\tau^-}\, f(\tau_{\tau i}) + g^P_{H_i l^+ l^-} g^P_{H_i\tau^+\tau^-}\, g(\tau_{\tau i})\right], \\
& - \frac{\alpha_{\rm em}\,m_l^2}{16\pi^3} \sum_{i=1}^{3} \frac{g^S_{H_i l^+ l^-}}{M^2_{H_i}} g_{H_i H^+ H^-}\, F(\tau_{H^\pm i}) \\
& + \frac{\alpha_{\rm em}^2\,m_l^2}{2\sqrt{2}\pi^2 s_W^2 M_W} \\
& \quad \times \sum_{i=1}^{3} \sum_{j=1,2} \frac{1}{m_{\chi_j^\pm}} \left[-g^S_{H_i l^+ l^-} g^S_{H_i\chi_j^+\chi_j^-}\, f(\tau_{\chi_j^\pm i}) + g^P_{H_i l^+ l^-} g^P_{H_i\chi_j^+\chi_j^-}\, g(\tau_{\chi_j^\pm i})\right],
\end{aligned} \tag{3.8}$$

[3]Here we add the contribution from the charged Higgs boson loop and confirm the positive signs of the fermionic Barr-Zee contributions [36].

where $\tau_{xi} = m_x^2/M_{H_i}^2$ and the two-loop functions $F(\tau)$, $f(\tau)$, and $g(\tau)$ are

$$\begin{aligned} F(\tau) &= \int_0^1 dx\, \frac{x(1-x)}{\tau - x(1-x)} \ln\left[\frac{x(1-x)}{\tau}\right], \\ f(\tau) &= \frac{\tau}{2}\int_0^1 dx\, \frac{1 - 2x(1-x)}{x(1-x) - \tau} \ln\left[\frac{x(1-x)}{\tau}\right], \\ g(\tau) &= \frac{\tau}{2}\int_0^1 dx\, \frac{1}{x(1-x) - \tau} \ln\left[\frac{x(1-x)}{\tau}\right]. \end{aligned} \tag{3.9}$$

For genuine SUSY contributions, the embedded SM contribution should be subtracted. We estimate the SM contributions as

$$(a_l)^H_{\rm SM} = -\sum_{q=t,b}\left[\frac{3\alpha_{\rm em}^2 Q_q^2 m_l^2}{4\pi^2 s_W^2 M_W^2} f(\tau_{q\rm SM})\right] - \frac{\alpha_{\rm em}^2 m_l^2}{4\pi^2 s_W^2 M_W^2} f(\tau_{\tau\rm SM})\,, \tag{3.10}$$

where $\tau_{f\rm SM} = m_f^2/M_{H_{\rm SM}}^2$. We find that $\left|(a_\mu)^H_{\rm SM}\right| \simeq 1.8\times 10^{-11}$ when $M_{H_{\rm SM}} = 100\,\text{GeV}$ and it decreases as $M_{H_{\rm SM}}$ increases. In our numerical analysis, we safely neglect $(a_l)^H_{\rm SM}$.

## 4 Numerical analysis

Adding up all the contributions considered in the previous sections and neglecting $(a_l)^H_{\rm SM}$, the supersymmetric contribution to the muon MDM is given by [32]

$$\begin{aligned} (a_\mu)_{\rm SUSY} &= \left(1 - \frac{4\alpha_{\rm em}}{\pi}\log\frac{M_{\rm SUSY}}{m_\mu}\right)\left[(a_\mu)^{\chi^\pm} + (a_\mu)^{\chi^0} + (a_\mu)^H\right] \\ &\equiv (a_\mu)^{\chi^\pm}_{\rm SUSY} + (a_\mu)^{\chi^0}_{\rm SUSY} + (a_\mu)^H_{\rm SUSY}\,, \end{aligned} \tag{4.1}$$

where the large QED logarithm takes into account the renormalization-group (RG) evolution of $a_\mu$ from the SUSY scale down to the muon-mass scale. The logarithmic correction amounts to -7 % and -9 % for $M_{\rm SUSY} = 100\,\text{GeV}$ and 1000 GeV, respectively.

### 4.1 A typical scenario where 1 loop dominates

We first consider a typical scenario in which the dominant contributions come from the one-loop chargino and neutralino diagrams [32]. We set

$$|\mu| = |M_2| = 2|M_1| = M_{\tilde L_2} = M_{\tilde E_2} = M_S\,. \tag{4.2}$$

The common scale $M_S$ and $\tan\beta$ are varied. For CP phases, we first consider the two values for $\Phi_\mu = 0^\circ$ or $180^\circ$ while taking vanishing CP phases for the gaugino mass and $A$ parameters: $\Phi_{1,2,3} = \Phi_A = 0^\circ$. The remaining relevant parameters are fixed as

$$\begin{aligned} M_{H^\pm} &= 300 \ \text{GeV}, \\ M_{\tilde Q_3} = M_{\tilde U_3} &= M_{\tilde D_3} = M_{\tilde L_3} = M_{\tilde E_3} = 0.5 \ \text{TeV}, \\ |A_{t,b,\tau}\,\mu| &= 1 \ \text{TeV}, \qquad |M_3| = 1 \ \text{TeV}\,. \end{aligned} \tag{4.3}$$

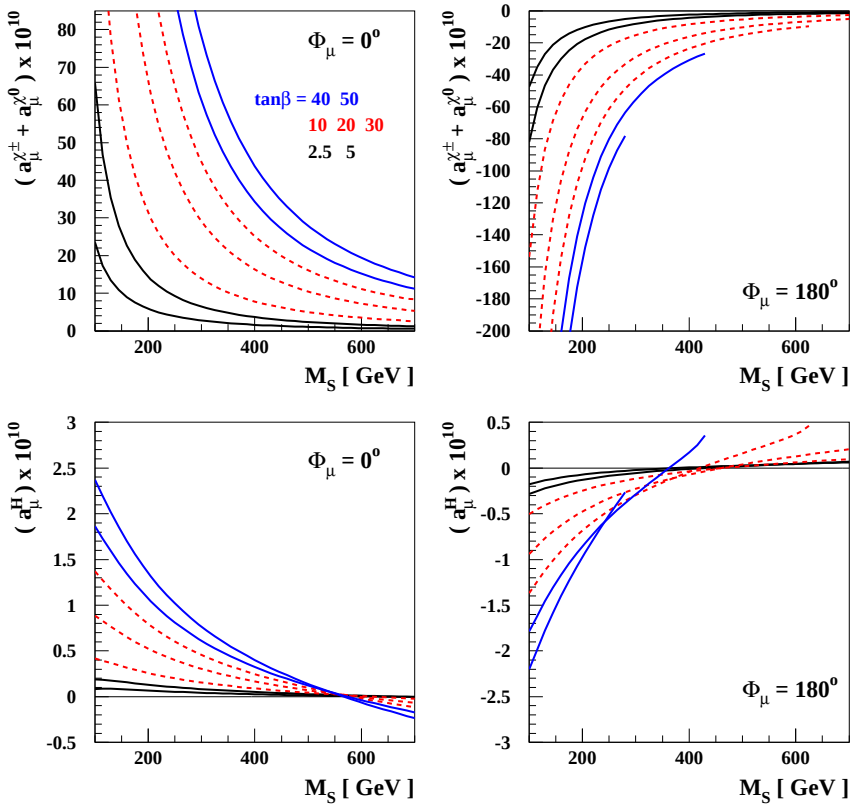


**Figure 3**. The one- (upper) and two-loop (lower) contributions to $(a_\mu)_{\rm SUSY}$ as functions of $M_S$ (4.2) for $\tan\beta = 2.5, 5, 10, 20, 30, 40, 50$. In all frames, the smaller value of $\tan\beta$ gives smaller $|a_\mu|$. The other parameters are chosen as in eq. (4.3).

In figure 3, we show the one-loop contributions from the chargino and neutralino diagrams (upper) and the two-loop contributions from the Barr-Zee graphs (lower) to the SUSY muon MDM as functions of $M_S$ for several values of $\tan\beta$. The left frames are for $\Phi_\mu = 0°$ and the right ones for $\Phi_\mu = 180°$. In both cases, the two-loop and one-loop contributions have same signs for most regions of $M_S$. The one-loop and two-loop contributions drops rapidly as $M_S$ increases. The case of $\Phi_\mu = 0°$ gives the correct sign and, for example, we have $(a_\mu)_{\rm SUSY} \times 10^{10} \gtrsim 10$ at $M_S = 500\,\text{GeV}$ when $\tan\beta \gtrsim 20$. For $\Phi_\mu = 180°$, $(a_\mu)_{\rm SUSY}$ is negative and the considered regions of $M_S$ are not allowed because data prefers a positive $a_\mu$. Note that for $\tan\beta \geq 30$, the $\tan\beta$-enhanced threshold corrections can turn the $b$-quark Yukawa coupling non-perturbative. This happens when $M_S$ (or $|\mu|$) is sufficiently large, as for the case at hand. It is shown by the termination of the curves in the right panels of figure 3. Our results are in good agreement with existing ones in literature.

Figure 4 shows the SUSY muon MDM (upper) and EDM (lower) as functions of $\Phi_2$ taking $\Phi_1 = 0°$ (left) and 180° (right). We have taken $\Phi_\mu = 0°$, $M_S = 250\,\text{GeV}$, $\tan\beta = 30$, and the other parameters the same as in figure 3. In both the MDM and EDM, we observe that the dominant contribution is coming from the one-loop chargino diagrams. The subleading contribution from the neutralino diagrams is about 5 to 10 times smaller and likely has an opposite sign with respect to the dominant chargino contribution. The contributions from the Higgs-mediated Barr-Zee diagrams are negligible. Numerically, we



JHEP06(2009)020

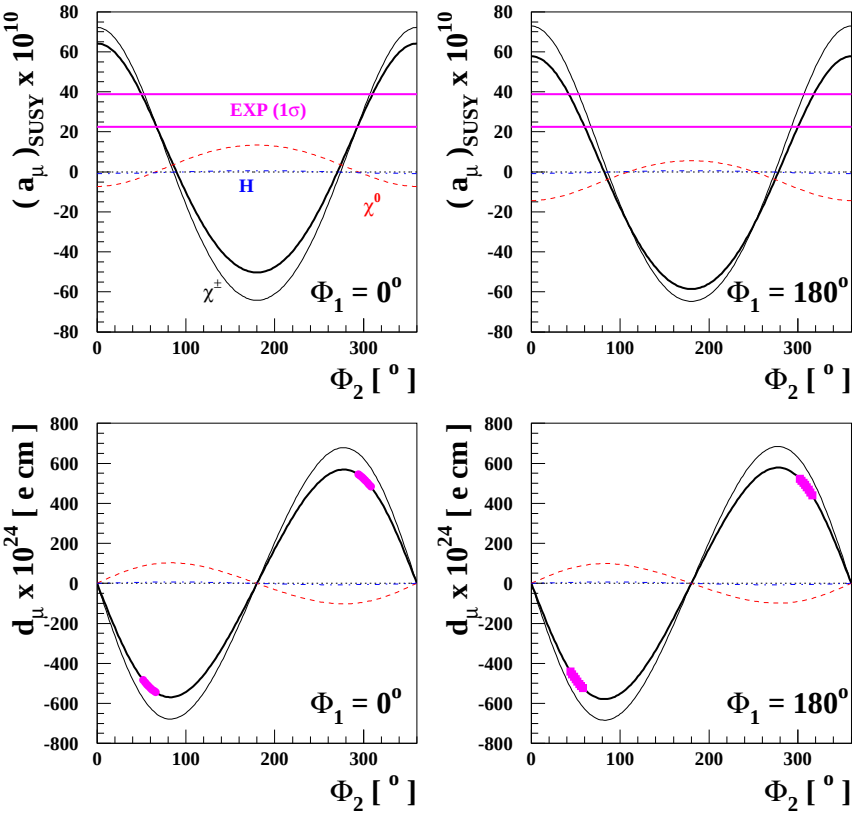


**Figure 4**. The MDM (upper) and EDM (lower) of the muon as functions of $\Phi_2$ taking $\Phi_1 = 0°$ (left) and 180° (right) when $\Phi_\mu = 0°$, $M_S = 250\,\text{GeV}$ and $\tan\beta = 30$. The thick line is for the total MDM/EDM and the thin solid, dashed, dash-dotted lines are for the constituent contributions from the one-loop chargino, the one-loop neutralino, and the two-loop Barr-Zee diagrams, respectively.

have $-0.8 < (a_\mu)^H_{\text{SUSY}} \times 10^{10} < 0.6$ and $|(d_\mu)^H| \times 10^{24} \lesssim 7\,e\,\text{cm}$. We clearly see the (shifted) cosine and sine functional forms of the MDM and EDM, respectively, as to be anticipated from the relations given in eq. (2.5). In the upper frames, the horizontal band is the experimental 1-$\sigma$-allowed region, $(30.7 \pm 8.2) \times 10^{10}$; see eq. (1.3). In the lower frames the region is overlayed with thick dots along the thick solid line. We note the chosen parameter set is compatible with the experimental data only for the non-trivial values of $\Phi_2$ around 60° and 300°, resulting in large EDM of about $\pm 5 \times 10^{-22}\,e\,\text{cm}$, which can be easily observed once the projected sensitivity of $10^{-24}$ can be achieved.

### 4.2 CPX scenario

Next we consider the CPX scenario [48]:

$$\begin{aligned} &M_{\tilde{Q}_3} = M_{\tilde{U}_3} = M_{\tilde{D}_3} = M_{\tilde{L}_3} = M_{\tilde{E}_3} = M_{\text{SUSY}}\,, \\ &|\mu| = 4\,M_{\text{SUSY}}\,, \qquad |A_{t,b,\tau}| = 2\,M_{\text{SUSY}}\,, \qquad |M_3| = 1\ \text{TeV}\,. \end{aligned} \tag{4.4}$$

Taking $A_\mu = A_\tau$, we fixed $\Phi_A = \Phi_3 = 90°$, $M_{\text{SUSY}} = 0.5\,\text{TeV}$, $|M_2| = 2|M_1| = 100\,\text{GeV}$ with $\Phi_{1,2} = 90°$, and $M_{\tilde{L}_2} = M_{\tilde{E}_2} = M_{\text{SUSY}}$. For our analysis, the most relevant feature



JHEP06(2009)020

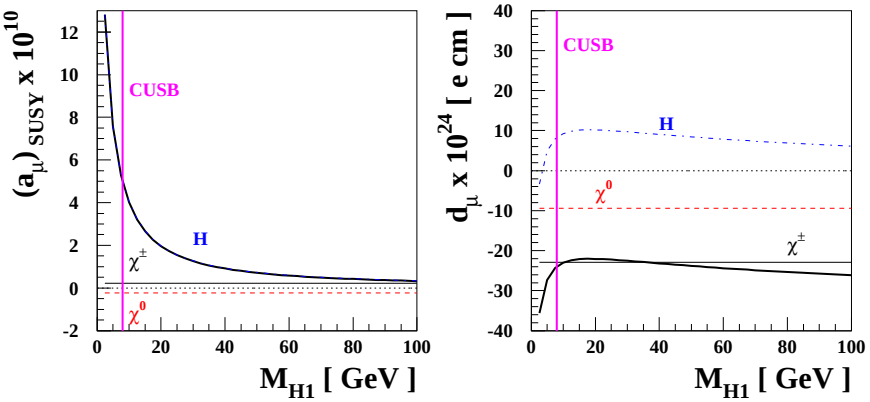


**Figure 5**. The muon SUSY MDM (left) and EDM (right) as functions of $M_{H_1}$ in the CPX scenario with $\tan\beta = 10$, see eq. (4.4). The lines are the same as in figure 4. In each frame, the region left to the vertical line is excluded by data on $\Upsilon(1S)$ decay [50].

of the scenario is that the combined searches of the four LEP collaborations reported two allowed regions where the lightest Higgs boson $H_1$ can be very light for moderate values of $3 \lesssim \tan\beta \lesssim 10$ [49]:

$$\begin{aligned} M_{H_1} &\lesssim 10 \text{ GeV} \qquad \text{for } 3 \lesssim \tan\beta \lesssim 10, \\ 30 \text{ GeV} \lesssim M_{H_1} &\lesssim 50 \text{ GeV} \qquad \text{for } 3 \lesssim \tan\beta \lesssim 10\,. \end{aligned} \tag{4.5}$$

On the other hand, a lower limit on the lightest Higgs boson, $M_{H_1} \gtrsim 8\,\text{GeV}$, is available from the bottomonium decay $\Upsilon(1S) \to \gamma H_1$ [50]. Figure 5 shows $(a_\mu)_{\rm SUSY}$ and $d_\mu$ in the CPX scenario as functions of $M_{H_1}$ taking $\tan\beta = 10$. When $M_{H_1} \lesssim 50\,\text{GeV}$, the one-loop contributions to $(a_\mu)_{\rm SUSY}$ are negligible compared to the Higgs-mediated two-loop contributions. The sign of $(a_\mu)^H_{\rm SUSY}$ is plus (+) since it is dominated by the bottom-quark and tau-lepton loops mediated by $H_1$ which is almost the CP odd state; see eq. (3.8). However, it is still difficult to achieve $(a_\mu)_{\rm SUSY} \times 10^{10} \gtrsim +10$ only with a mostly CP-odd Higgs boson as light as $\sim 8\,\text{GeV}$. For the EDM, the one- and two-loop contributions are comparable and tend to cancel each other.

### 4.3 An extreme scenario

Finally, we consider a scenario in which the one-loop neutralino and chargino contributions are suppressed while the two-loop Barr-Zee contributions dominate. This scenario is characterized by large $\tan\beta$, a light charged Higgs boson, very heavy smuons and muon sneutrinos, and very large $|\mu|$ and $|A_{b,\tau}|$ parameters. Explicitly, we have chosen

$$\begin{aligned} &\tan\beta = 50, \qquad M_{H^\pm} = 0.2 \text{ TeV}, \\ &M_{\tilde{L}_2} = M_{\tilde{E}_2} = 10 \text{ TeV}, \\ &M_{\tilde{Q}_3} = M_{\tilde{U}_3} = M_{\tilde{D}_3} = M_{\tilde{L}_3} = M_{\tilde{E}_3} = 1 \text{ TeV}, \\ &|A_t| = 1 \text{ TeV}, \qquad |M_2| = 2\,|M_1| = 0.1 \text{ TeV}, \qquad |M_3| = 1 \text{ TeV}, \\ &\Phi_\mu = 0^\circ\,, \qquad \Phi_{A_t} = 0^\circ\,, \qquad \Phi_{1,2} = 0^\circ\,, \end{aligned} \tag{4.6}$$



JHEP06(2009)020

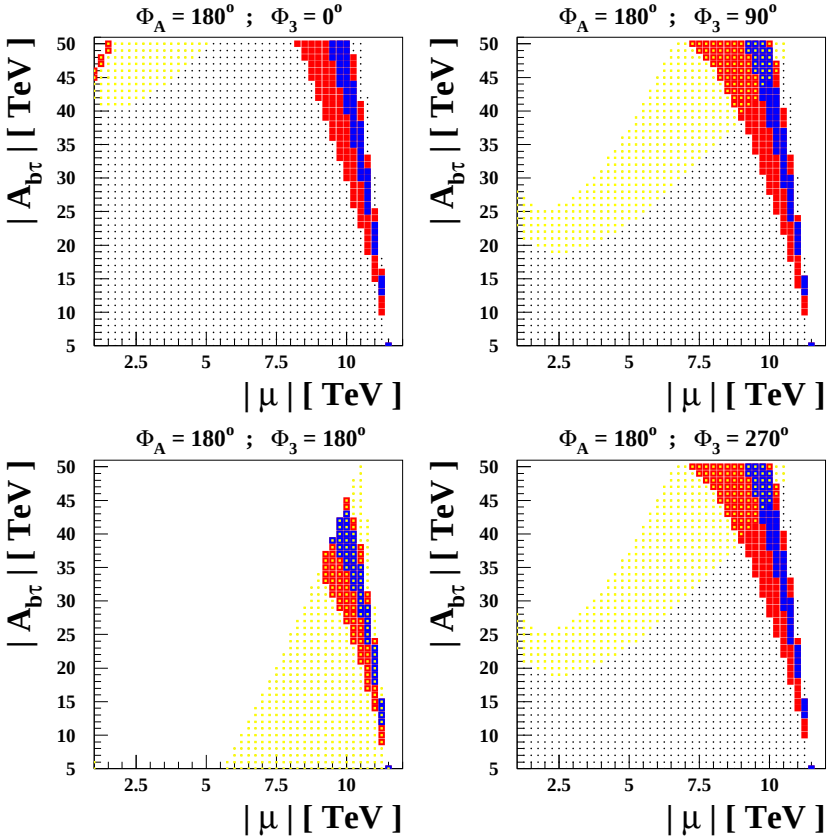


**Figure 6**. Allowed region at the 1-$\sigma$ (blue) and 2-$\sigma$ (blue+red) level in the $|A_{b\tau}|$ and $|\mu|$ plane, see eq. (1.3), for $\Phi_3 = 0°$ (upper-left), 90° (upper-right), 180° (lower-left), and 270° (lower-right). We have taken $\Phi_{A_{b\tau}} = 180°$. The unshaded regions are not theoretically allowed and $M_{H_1} < 100\,\text{GeV}$ in the over-shaded regions (yellow). See eq. (4.6) for other parameters chosen.

while varying

$$\Phi_{A_{b\tau}}\,, \quad \Phi_3\,; \quad 1 < |\mu|/\text{TeV} < 12\,, \quad 1 < |A_{b\tau}|/\text{TeV} < 50\,. \tag{4.7}$$

where $|A_{b\tau}| \equiv |A_b| = |A_\tau|$ and we have taken $A_\mu = A_\tau$. Note $|A_t|$ is fixed in this scenario and the results are almost independent of $\Phi_{1,2}$.

Figure 6 shows the regions where $(a_\mu)_{\text{SUSY}} = 30.2 \pm 8.8$ (blue) and $(a_\mu)_{\text{SUSY}} = 30.2 \pm 17.6$ (blue+red) in the $|A_{b\tau}|$ and $|\mu|$ plane for several values of $\Phi_3$, taking $\Phi_{A_{b\tau}} = 180°$. The unshaded regions are not theoretically allowed and we have $M_{H_1} < 100\,\text{GeV}$ in the over-shaded regions (yellow), for example, in the upper-left corner in the upper-left frame. We found that $H_1$ is always lighter than 100 GeV when $\Phi_3 = 180°$ (lower-left) because the resummed threshold corrections modify the bottom-quark Yukawa coupling significantly in this case. We note the region with larger $|A_{b\tau}|$ is more preferred. Figure 7 shows the dependence on $\Phi_{A_{b\tau}}$ of $(a_\mu)_{\text{SUSY}}$, $d_\mu$, and the masses of the lighter stau and the lightest Higgs boson. In the upper-left frame, the horizontal band is the experimental 1-$\sigma$ region of $\Delta a_\mu^{\text{EXP}}$. We found $150° \lesssim \Phi_{A_{b\tau}} \lesssim 210°$ and $\Phi_{A_{b\tau}} \sim 140°\,, 220°$ can make $(a_\mu)_{\text{SUSY}}$ consis-



JHEP06(2009)020

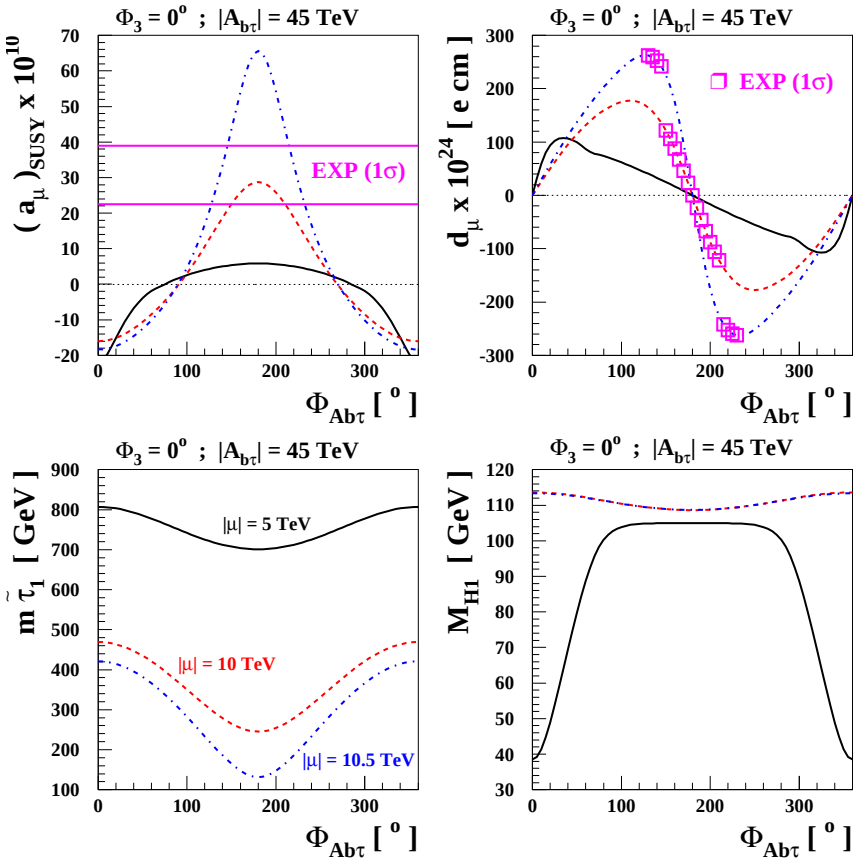


**Figure 7**. Dependence on $\Phi_{A_{b\tau}}$ of $(a_\mu)_{\rm SUSY}$ (upper-left), $d_\mu$ (upper-right), and the masses of the lighter stau (lower-left) and $H_1$ (lower-right) for three values of $\mu$: 5 TeV (solid), 10 TeV (dashed), and 10.5 TeV (dashed-dotted). We have taken $\Phi_3 = 0^\circ$ and $|A_{b\tau}| = 45$ TeV. See eq. (4.6) for other parameters chosen.

tent with the experimental value for $|\mu| = 10$ TeV and 10.5 TeV, respectively. In the upper-right frame, the 1-$\sigma$ region is overlayed with blank boxes along the dashed ($|\mu| = 10$ TeV) and dash-dotted ($|\mu| = 10.5$ TeV) lines. We have $|d_\mu| \times 10^{24} \lesssim 120\, e$ cm and $d_\mu \times 10^{24} \sim \pm 250\, e$ cm for $|\mu| = 10$ TeV and 10.5 TeV, respectively. We observe that the larger $|\mu|$ results in the lighter staus as shown in the lower-left frame. This leads to a larger $(a_\mu)_{\rm SUSY}$ as the dominant contribution in this case comes from the Higgs-mediated stau Barr-Zee graphs, as will be shown later. When $|\mu| = 5$ TeV, $H_1$ becomes lighter than 100 GeV for $\Phi_{A_{b\tau}} \lesssim 80^\circ$ and $\gtrsim 280^\circ$, as shown in the lower-right frame. When $|\mu| \geq 10$ TeV, $M_{H_1} \gtrsim 108$ GeV.

Figure 8 shows the dependence of $(a_\mu)_{\rm SUSY}$ on $|\mu|$ (upper-left) and $|A_{b\tau}|$ (upper-right) for several values of $|A_{b\tau}|$ and $|\mu|$, respectively, taking $\Phi_{A_{b\tau}} = 180^\circ$ and $\Phi_3 = 0^\circ$. In the lower frames we also show the dependence of the mass of the lighter stau $\tilde{\tau}_1$. Again we observe that large $|\mu|$ and $|A_{b\tau}|$ can easily make $(a_\mu)_{\rm SUSY}$ consistent with the current $\Delta a_\mu^{\rm EXP}$. Figure 9 shows various constituent as well as the total two-loop Barr-Zee contributions to the muon MDM $(a_\mu)^H_{\rm SUSY}$, as functions of $|\mu|$ taking $|A_{b\tau}| = 40$ TeV, $\Phi_{A_{b\tau}} = 180^\circ$ and $\Phi_3 = 0^\circ$. The thick line is for the total and the thin lines are for the constituent eight



JHEP06(2009)020

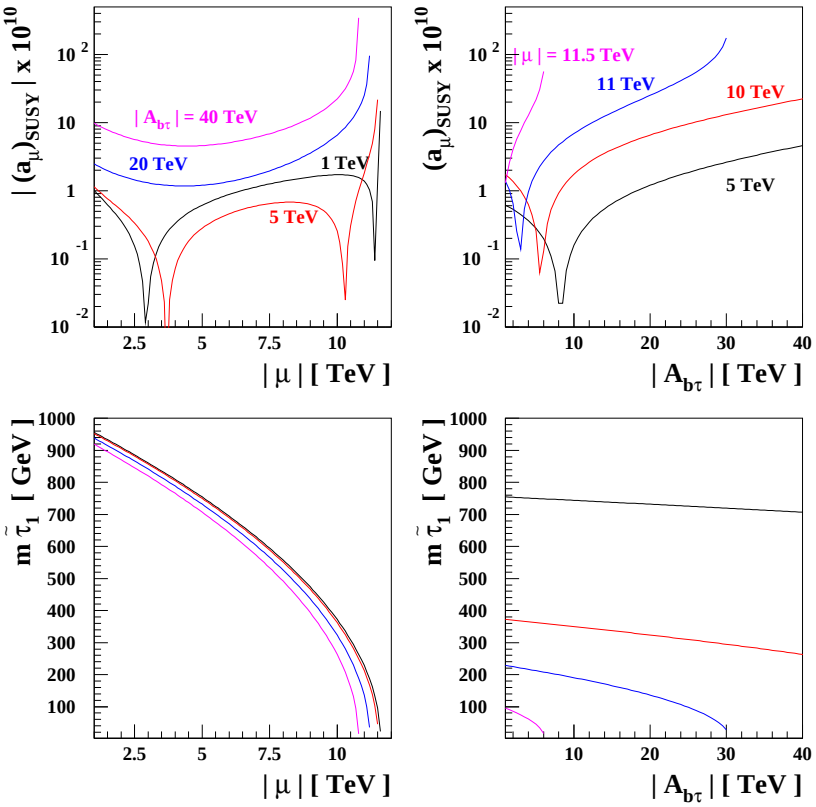


**Figure 8**. Dependence of $(a_\mu)_{\rm SUSY}$ on $|\mu|$ (upper-left) and $|A_{b\tau}|$ (upper-right) for several values of $|A_{b\tau}|$ and $|\mu|$, respectively, taking $\Phi_{A_{b\tau}} = 180°$ and $\Phi_3 = 0°$. The regions of $|\mu|$ and $|A_{b\tau}|$ are constrained by applying the experimental limit on the lightest stau mass as shown below. The lines are the same as in the upper frames. See eq. (4.6) for other parameters chosen.

contributions (see figure 2). For smaller $|\mu|$, the dominant contribution comes from the charged Higgs boson loop. This is because the $H_i$-$H^+$-$H^-$ couplings have loop-induced enhancement from large $|A_b|$ and $|\mu|$ [51]. The possibility of such a significant contribution of the (photon-)Barr-Zee diagram with a (closed) charged Higgs boson loop has apparently not been noticed before. In fact, the particular diagram is typically not included in analyses at more or less the same level of numerical precision to ours presented here. As $|\mu|$ grows, however, the contribution from the stau loops is enhanced and thus becomes dominant. The contribution from the sbottom loop is not significant because the resummed threshold corrections suppress the bottom-quark Yukawa coupling for the chosen parameter set.

The scenario likely seems too contrived to some readers. However, we are presenting it here mainly to illustrate the significant roles of the various two-loop Barr-Zee contributions in some region of the parameter space. While the dominance of the latter group reduces as one moves away from the extreme corner of the parameter space, its significance maintains over a substantial region. For instance, we show the dependence of $(a_\mu)_{\rm SUSY}$ on $M_{\tilde{L}_2,\tilde{E}_2}$ and $|\mu|$ in figure 10, i.e. the effect of bringing back the smuon mass from the heavy limit. In particular, the Higgs-mediated two-loop Barr-Zee contributions are shown to be actually



JHEP06(2009)020

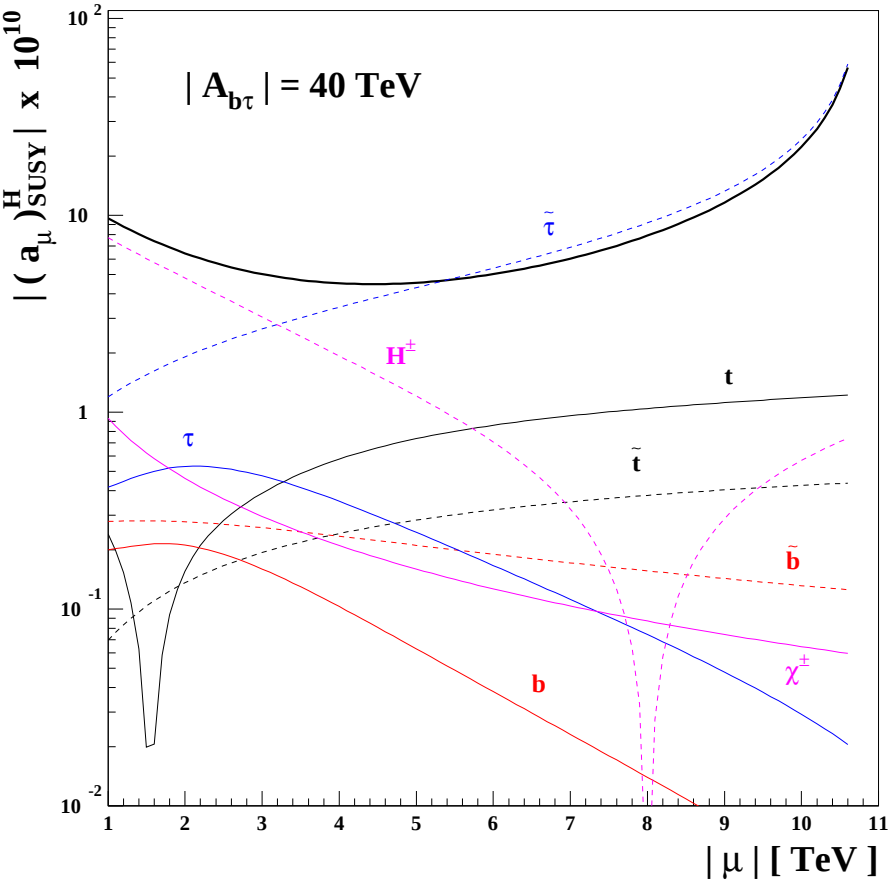


**Figure 9**. The Barr-Zee contributions to $(a_\mu)_{\rm SUSY}$, $(a_\mu)^H_{\rm SUSY}$, as functions of $|\mu|$ taking $|A_{b\tau}| = 40\,\text{TeV}$, $\Phi_{A_{b\tau}} = 180^\circ$ and $\Phi_3 = 0^\circ$. Also shown are the constituent contribution from the eight types of diagrams. See eq. (4.6) for other parameters chosen.

dominate over the one-loop contributions even when the smuon mass parameters get down to as low as 1 TeV (left), for the full range of $|\mu|$ values (right).

Before closing this section, we comment on the relation between the muon and electron EDMs. The most important one-loop contribution $(d_l)^\chi$ and that from the two-loop $(d_l)^H$ have somewhat different features. The Barr-Zee diagrams for the muon and the electron are identical except for the muon and the electron lines themselves. Hence, we have the robust relation

$$(d_e)^H = (m_e/m_\mu)\,(d_\mu)^H\,. \tag{4.8}$$

For the case of $(d_l)^\chi$, however, it is sensitive to the flavor dependence of the soft SUSY breaking terms. In most of the models on the origin of the soft SUSY breaking terms available in the literature, those of the first two generations are more or less the same. Explicitly,

$$M_{\tilde{L}_1} \sim M_{\tilde{L}_2}\,, \qquad M_{\tilde{E}_1} \sim M_{\tilde{E}_2}\,, \qquad A_e \sim A_\mu\,.$$

That does give us a relation

$$(d_e)^\chi \sim (m_e/m_\mu)\,(d_\mu)^\chi\,, \tag{4.9}$$



JHEP06(2009)020

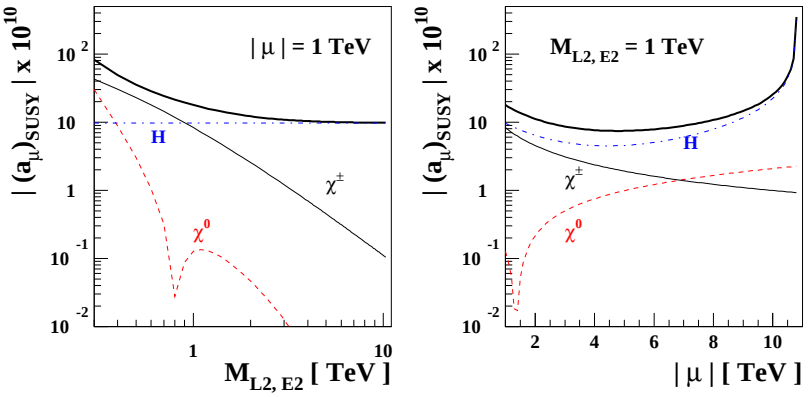


**Figure 10**. Dependence of $(a_\mu)_{\rm SUSY}$ on $M_{\tilde{L}_2,\tilde{E}_2}$ (left) and $|\mu|$ (right) for fixed values of $|\mu|$ and $M_{\tilde{L}_2,\tilde{E}_2}$. The thick line is for the total and the thin solid (black), dashed (red), and dash-dotted (blue) lines are for the constituent contributions from the one-loop chargino, one-loop neutralino, and Higgs-mediated two-loop Barr-Zee diagrams. See eq. (4.6) for other parameters chosen.

which is particularly sensitive to the CP phases of the $A_e$ and $A_\mu$ parameters. To summarize, one may consider special cases with $(i)$ similar or universal soft terms (for electron and muon) or $(ii)$ electron EDM dominated by the two-loop Barr-Zee graphs, $d_e \sim (d_e)^H$, possibly due to much heavier selectron masses. Depending on situations, $d_\mu \sim (d_\mu)^\chi + (d_\mu)^H$ or $(d_\mu)^H$ is very strongly constrained by the Thallium EDM as

$$(i)\ \ |d_\mu| < 3\times 10^{-25}\, e\,\text{cm} \qquad ; \qquad (ii)\ \ |(d_\mu)^H| < 3\times 10^{-25}\, e\,\text{cm}\,, \tag{4.10}$$

where we used $m_e/m_\mu = 1/213$, $d_{\rm Tl} \simeq -585\cdot d_e$ and $|d_{\rm Tl}| < 9\times 10^{-25}\, e\,\text{cm}$ [38]. Note that these limits are model dependent and the muon EDM should be measured independently of the Thallium EDM.

## 5 Conclusions

We have studied in detail various supersymmetric contributions to muon MDM and EDM, including one-loop chargino and neutralino diagrams and dominant two-loop Barr-Zee diagrams. In general, the one-loop contributions dominate over the two-loop contributions, however there are interesting regions of the model parameter space where the two-loop Barr-Zee diagrams are the major source of contributions to muon MDM and/or EDM. The model parameter space is huge. It is not feasible for us to present and discuss here the numerical results for more than a few cases of interest. We try to pick cases that can illustrate the essential and interesting features, and leave it mostly to the readers to project onto the parameter space regions in between, or considered otherwise to be of special interest. We illustrate numerically 3 scenarios under various choices of soft parameters: (i) the one when the one-loop contributions dominate, (ii) the CPX in which the Barr-Zee dominates but the overall sizes of MDM and EDM are small, and (iii) a more exotic one in which the Barr-Zee dominates and the overall sizes of MDM and EDM are large. We have also shown interesting relations between the MDM and EDM. For the case when one-loop



JHEP06(2009)020

contributions dominate the MDM and EDM are just, respectively, the (shifted) cosines and sines of the phase of the parameters involved. Existing experimentally preferred range of MDM already predicts an interesting range of EDM, which can be further tested in the future muon EDM experiments. For the case the MDM is dominated by two-loop Barr-Zee contributions the MDM and EDM can be connected by the relation in eq. (3.7) — a result of the more complicated Higgs sector phase structure.

The CPX scenario may still allow a light Higgs boson after taking into account all the existing search limits. Potentially, the light Higgs boson could give large enhancement to muon MDM. However, after imposing the lower limit on $M_{H_1}$ the resulting MDM is always less than $5 \times 10^{-10}$, which is smaller than the experimentally favored value.

The last scenario associated with large $\tan\beta$, large $|\mu|$, heavy smuons and muon sneutrinos, and large $|A_{b\tau}|$ but light charged Higgs boson and stau is rather interesting. It suppresses the one-loop contributions but the two-loop contributions are large enough to explain the muon MDM data, which are dominated by charged Higgs boson and stau at smaller and larger $|\mu|$, respectively. For large enough $|\mu|$ the MDM data can be accommodated easily. The particular interesting role of the charged Higgs boson escaped earlier studies. We have also illustrated that major features of the scenario persist over a region of the parameter space with milder conditions — in particular, more 'regular' smuon masses.

In addition, we offer the following comments.

1. We have included the threshold corrections to Yukawa couplings. In particular, the bottom-quark Yukawa can receive large corrections at large $\tan\beta$ with large $|M_3|$ and $|\mu|$. For $\tan\beta \gtrsim 30$ the threshold corrections can make the $b$-quark Yukawa coupling turn non-perturbative when $M_S$ (or $|\mu|$) is sufficiently large.

2. The one-loop contributions to MDM and EDM can vary as shifted cosines and sines of the phase of the parameters.

3. As shown in figure 4, the prediction for EDM is of order $500 \times 10^{-24}\, e$ cm within the allowed range of MDM. It is about $2-3$ orders of magnitude below the current limit, but will be within reach of future muon EDM experiments [41].

4. The CPX scenario may still allow a $H_1$ as light as a few to tens of GeVs. It could be searched in the subsequent decay of the $H_2 \to H_1 H_1$, where $H_2$ is the SM-like Higgs boson. The contribution of $H_1$ to the muon EDM has a right sign but it may not be large enough to accommodate $\Delta a_\mu^{\rm EXP}$ after taking account of the constraint from the bottomonium decay $\Upsilon(1S) \to \gamma H_1$.

5. The last scenario that we studied is characterized by a very light stau, a light bino and wino, a light $M_{H_1}$, and a light charged Higgs boson. The predicted EDM is from 0 to $100 \times 10^{-24}\, e\,$cm. Experimental searches for this scenario at the LHC will be a lot of tau leptons in the final state because of lightness of stau.

6. The parameter space compatible with the $\Delta a_\mu^{\rm EXP}$ value required is generally extended by allowing CP phases. For example, in figure 4: the CP-conserving cases ($\Phi_2 = 0^\circ$ and $180^\circ$) are excluded.



JHEP06(2009)020

## Acknowledgments

We thank Dominik Stöckinger and Apostolos Pilaftsis for helpful discussions. We also thank Joaquim Prades for valuable information on the hadronic light-by-light contributions. The work was partially supported by the NSC of Taiwan (96-2112-M-008-007-MY3), the Boost Project of NTHU, and the WCU program through the KOSEF funded by the MEST (R31-2008-000-10057-0).

## A `CPsuperH` interface

- Output: For output, part of auxiliary array `RAUX_H` is used.
  - The muon EDM in units of $cm$:

$$\texttt{RAUX\_H(360)} = d_\mu/e = (d_\mu/e)^{\tilde{\chi}^\pm} + (d_\mu/e)^{\tilde{\chi}^0} + (d_\mu/e)^{\tilde{g}} + (d_\mu/e)^{H}\,, \qquad \text{(A.1)}$$

    where the sub-contributions are

$$\begin{aligned} \texttt{RAUX\_H(361)} &= (d_\mu/e)^{\tilde{\chi}^\pm}\,, \quad \texttt{RAUX\_H(362)} = (d_\mu/e)^{\tilde{\chi}^0} \\ \texttt{RAUX\_H(363)} &= (d_\mu/e)^{\tilde{g}}\,, \quad \texttt{RAUX\_H(364)} = (d_\mu/e)^{H}\,. \end{aligned}$$

  - The muon MDM:

$$\texttt{RAUX\_H(380)} = (a_\mu)_{\rm SUSY} = (a_\mu)^{\tilde{\chi}^\pm}_{\rm SUSY} + (a_\mu)^{\tilde{\chi}^0}_{\rm SUSY} + (a_\mu)^{\tilde{g}}_{\rm SUSY} + (a_\mu)^{H}_{\rm SUSY}\,, \quad \text{(A.2)}$$

    where the sub-contributions are

$$\begin{aligned} \texttt{RAUX\_H(381)} &= (a_\mu)^{\tilde{\chi}^\pm}_{\rm SUSY}\,, \quad \texttt{RAUX\_H(382)} = (a_\mu)^{\tilde{\chi}^0}_{\rm SUSY} \\ \texttt{RAUX\_H(383)} &= (a_\mu)^{\tilde{g}}_{\rm SUSY}\,, \quad \texttt{RAUX\_H(384)} = (a_\mu)^{H}_{\rm SUSY}\,. \end{aligned}$$

- `IFLAG_H(19)`=1 is used to print out EDM/MDM of the muon. Using `run` shell-script file distributed, the sample out obtained is

```
-------------------------------------------------------
The Electric EDM of muon in cm:
-------------------------------------------------------
    d^E_mu/e[Total]:  0.1288E-23
 d^E_mu/e[C,N,Gl,H]:  0.0000E+00  -.6035E-24  0.0000E+00  0.1891E-23
-------------------------------------------------------
The SUSY MDM of muon:
-------------------------------------------------------
        a_mu[Total]:  0.1805E-09
     a_mu[C,N,Gl,H]:  0.1396E-09  0.2871E-10  0.0000E+00  0.1218E-10
-------------------------------------------------------
```

## References


[1] R.M. Carey et al., *New measurement of the anomalous magnetic moment of the positive muon*, *Phys. Rev. Lett.* **82** (1999) 1632 [SPIRES];
Muon (g-2) collaboration, H.N. Brown et al., *Improved measurement of the positive muon anomalous magnetic moment*, *Phys. Rev.* **D 62** (2000) 091101 [hep-ex/0009029] [SPIRES];
*Precise measurement of the positive muon anomalous magnetic moment*, *Phys. Rev. Lett.* **86** (2001) 2227 [hep-ex/0102017] [SPIRES];
Muon g-2 collaboration, G.W. Bennett et al., *Measurement of the positive muon anomalous magnetic moment to 0.7 ppm*, *Phys. Rev. Lett.* **89** (2002) 101804 [*Erratum ibid.* **89** (2002) 129903] [hep-ex/0208001] [SPIRES]; *Measurement of the negative muon anomalous magnetic moment to 0.7 ppm*, *Phys. Rev. Lett.* **92** (2004) 161802 [hep-ex/0401008] [SPIRES]; *Final report of the muon E821 anomalous magnetic moment measurement at BNL*, *Phys. Rev.* **D 73** (2006) 072003 [hep-ex/0602035] [SPIRES].

[2] M. Passera, W.J. Marciano and A. Sirlin, *The muon $g-2$ discrepancy: errors or new physics?*, *AIP Conf. Proc.* **1078** (2009) 378 [arXiv:0809.4062] [SPIRES];
F. Jegerlehner and A. Nyffeler, *The muon $g-2$*, arXiv:0902.3360 [SPIRES];
J.P. Miller, E. de Rafael and B.L. Roberts, *Muon $g-2$: review of theory and experiment*, *Rept. Prog. Phys.* **70** (2007) 795 [hep-ph/0703049] [SPIRES];
F. Jegerlehner, *Essentials of the muon $g-2$*, *Acta Phys. Polon.* **B 38** (2007) 3021 [hep-ph/0703125] [SPIRES].

[3] T. Kinoshita and M. Nio, *Improved $\alpha^4$ term of the muon anomalous magnetic moment*, *Phys. Rev.* **D 70** (2004) 113001 [hep-ph/0402206] [SPIRES]; *Improved $\alpha^4$ term of the electron anomalous magnetic moment*, *Phys. Rev.* **D 73** (2006) 013003 [hep-ph/0507249] [SPIRES]; *The tenth-order QED contribution to the lepton $g-2$: evaluation of dominant $\alpha^5$ terms of muon $g-2$*, *Phys. Rev.* **D 73** (2006) 053007 [hep-ph/0512330] [SPIRES];
T. Aoyama, M. Hayakawa, T. Kinoshita and M. Nio, *Revised value of the eighth-order electron $g-2$*, *Phys. Rev. Lett.* **99** (2007) 110406 [arXiv:0706.3496] [SPIRES]; *Revised value of the eighth-order QED contribution to the anomalous magnetic moment of the electron*, *Phys. Rev.* **D 77** (2008) 053012 [arXiv:0712.2607] [SPIRES].

[4] S. Laporta and E. Remiddi, *The analytical value of the electron light-light graphs contribution to the muon $(g-2)$ in QED*, *Phys. Lett.* **B 301** (1993) 440 [SPIRES]; *The analytical value of the electron $(g-2)$ at order $\alpha^3$ in QED*, *Phys. Lett.* **B 379** (1996) 283 [hep-ph/9602417] [SPIRES].

[5] M. Passera, *Precise mass-dependent QED contributions to leptonic $g-2$ at order $\alpha^2$ and $\alpha^3$*, *Phys. Rev.* **D 75** (2007) 013002 [hep-ph/0606174] [SPIRES];
A.L. Kataev, *Reconsidered estimates of the 10th order QED contributions to the muon anomaly*, *Phys. Rev.* **D 74** (2006) 073011 [hep-ph/0608120] [SPIRES].

[6] A. Czarnecki, B. Krause and W.J. Marciano, *Electroweak Fermion loop contributions to the muon anomalous magnetic moment*, *Phys. Rev.* **D 52** (1995) 2619 [hep-ph/9506256] [SPIRES]; *Electroweak corrections to the muon anomalous magnetic moment*, *Phys. Rev. Lett.* **76** (1996) 3267 [hep-ph/9512369] [SPIRES];
A. Czarnecki, W.J. Marciano and A. Vainshtein, *Refinements in electroweak contributions to the muon anomalous magnetic moment*, *Phys. Rev.* **D 67** (2003) 073006 [*Erratum ibid.* **D 73** (2006) 119901] [hep-ph/0212229] [SPIRES].

[7] M. Davier, *The hadronic contribution to $(g-2)_\mu$*, *Nucl. Phys. Proc. Suppl.* **169** (2007) 288 [hep-ph/0701163] [SPIRES];




JHEP06(2009)020

S. Eidelman, *Status of* $(g_\mu - 2)/2$ *in standard model*, *Acta Phys. Polon.* **B 38** (2007) 3015 [SPIRES].

[8] K. Hagiwara, A.D. Martin, D. Nomura and T. Teubner, *Improved predictions for* $g-2$ *of the muon and* $\alpha_{\rm QED}(M_Z^2)$, *Phys. Lett.* **B 649** (2007) 173 [hep-ph/0611102] [SPIRES].

[9] F. Jegerlehner, *Precision measurements of* $\sigma_{\rm hadronic}$ *for* $\alpha_{\rm eff}(E)$ *at ILC energies and* $(g-2)_\mu$, *Nucl. Phys. Proc. Suppl.* **162** (2006) 22 [hep-ph/0608329] [SPIRES].

[10] J.F. de Troconiz and F.J. Yndurain, *The hadronic contributions to the anomalous magnetic moment of the muon*, *Phys. Rev.* **D 71** (2005) 073008 [hep-ph/0402285] [SPIRES].

[11] F. Jegerlehner, *Muon* $g-2$ *update*, *Nucl. Phys. Proc. Suppl.* **181-182** (2008) 26 [SPIRES].

[12] B. Krause, *Higher-order hadronic contributions to the anomalous magnetic moment of leptons*, *Phys. Lett.* **B 390** (1997) 392 [hep-ph/9607259] [SPIRES].

[13] M. Knecht and A. Nyffeler, *Hadronic light-by-light corrections to the muon* $g-2$*: the pion-pole contribution*, *Phys. Rev.* **D 65** (2002) 073034 [hep-ph/0111058] [SPIRES];
M. Knecht, A. Nyffeler, M. Perrottet and E. de Rafael, *Hadronic light-by-light scattering contribution to the muon* $g-2$*: an effective field theory approach*, *Phys. Rev. Lett.* **88** (2002) 071802 [hep-ph/0111059] [SPIRES].

[14] K. Melnikov and A. Vainshtein, *Hadronic light-by-light scattering contribution to the muon anomalous magnetic moment revisited*, *Phys. Rev.* **D 70** (2004) 113006 [hep-ph/0312226] [SPIRES].

[15] J. Bijnens and J. Prades, *The hadronic light-by-light contribution to the muon anomalous magnetic moment: where do we stand?*, *Mod. Phys. Lett.* **A 22** (2007) 767 [hep-ph/0702170] [SPIRES].

[16] A. Nyffeler, *Hadronic light-by-light scattering in the muon* $g-2$*: a new short-distance constraint on pion-exchange*, arXiv:0901.1172 [SPIRES].

[17] J. Prades, E. de Rafael and A. Vainshtein, *Hadronic light-by-light scattering contribution to the muon anomalous magnetic moment*, arXiv:0901.0306 [SPIRES].

[18] D.K. Hong and D. Kim, *Pseudo scalar contributions to light-by-light correction of muon* $g-2$ *in AdS/QCD*, arXiv:0904.4042 [SPIRES].

[19] J.A. Grifols and A. Mendez, *Constraints on supersymmetric particle masses from* $(g-2)_\mu$, *Phys. Rev.* **D 26** (1982) 1809 [SPIRES];
J.R. Ellis, J.S. Hagelin and D.V. Nanopoulos, *Spin 0 leptons and the anomalous magnetic moment of the muon*, *Phys. Lett.* **B 116** (1982) 283 [SPIRES];
R. Barbieri and L. Maiani, *The muon anomalous magnetic moment in broken supersymmetric theories*, *Phys. Lett.* **B 117** (1982) 203 [SPIRES].

[20] D.A. Kosower, L.M. Krauss and N. Sakai, *Low-energy supergravity and the anomalous magnetic moment of the muon*, *Phys. Lett.* **B 133** (1983) 305 [SPIRES];
T.C. Yuan, R.L. Arnowitt, A.H. Chamseddine and P. Nath, *Supersymmetric electroweak effects on* $(g-2)_\mu$, *Zeit. Phys.* **C 26** (1984) 407 [SPIRES];
J.C. Romao, A. Barroso, M.C. Bento and G.C. Branco, *Flavor violation in supersymmetric theories*, *Nucl. Phys.* **B 250** (1985) 295 [SPIRES];
I. Vendramin, *Constraints on supersymmetric parameters from muon magnetic moment*, *Nuovo Cim.* **A 101** (1989) 731 [SPIRES].

[21] S.A. Abel, W.N. Cottingham and I.B. Whittingham, *The muon magnetic moment in flipped* SU(5), *Phys. Lett.* **B 259** (1991) 307 [SPIRES];

JHEP06(2009)020

J.L. Lopez, D.V. Nanopoulos and X. Wang, *Large* $(g-2)_\mu$ *in* SU(5) × U(1) *supergravity models*, *Phys. Rev.* **D 49** (1994) 366 [hep-ph/9308336] [SPIRES];
U. Chattopadhyay and P. Nath, *Probing supergravity grand unification in the Brookhaven* $g-2$ *experiment*, *Phys. Rev.* **D 53** (1996) 1648 [hep-ph/9507386] [SPIRES].

[22] T. Moroi, *The muon anomalous magnetic dipole moment in the minimal supersymmetric standard model*, *Phys. Rev.* **D 53** (1996) 6565 [*Erratum ibid.* **D56** (1997) 4424] [hep-ph/9512396] [SPIRES].

[23] G.-C. Cho, K. Hagiwara and M. Hayakawa, *Muon* $g-2$ *and precision electroweak physics in the MSSM*, *Phys. Lett.* **B 478** (2000) 231 [hep-ph/0001229] [SPIRES].

[24] S.P. Martin and J.D. Wells, *Muon anomalous magnetic dipole moment in supersymmetric theories*, *Phys. Rev.* **D 64** (2001) 035003 [hep-ph/0103067] [SPIRES].

[25] S. Heinemeyer, D. Stöckinger and G. Weiglein, *Two-loop SUSY corrections to the anomalous magnetic moment of the muon*, *Nucl. Phys.* **B 690** (2004) 62 [hep-ph/0312264] [SPIRES].

[26] S. Heinemeyer, D. Stöckinger and G. Weiglein, *Electroweak and supersymmetric two-loop corrections to* $(g-2)_\mu$, *Nucl. Phys.* **B 699** (2004) 103 [hep-ph/0405255] [SPIRES].

[27] G. Degrassi and G.F. Giudice, *QED logarithms in the electroweak corrections to the muon anomalous magnetic moment*, *Phys. Rev.* **D 58** (1998) 053007 [hep-ph/9803384] [SPIRES].

[28] T.-F. Feng, X.-Q. Li, L. Lin, J. Maalampi and H.-S. Song, *The two-loop supersymmetric corrections to lepton anomalous magnetic and electric dipole moments*, *Phys. Rev.* **D 73** (2006) 116001 [hep-ph/0604171] [SPIRES].

[29] S. Marchetti, S. Mertens, U. Nierste and D. Stöckinger, $\tan\beta$*-enhanced supersymmetric corrections to the anomalous magnetic moment of the muon*, *Phys. Rev.* **D 79** (2009) 013010 [arXiv:0808.1530] [SPIRES].

[30] T.-F. Feng, L. Sun and X.-Y. Yang, *Electroweak and supersymmetric two-loop corrections to lepton anomalous magnetic and electric dipole moments*, *Nucl. Phys.* **B 800** (2008) 221 [arXiv:0805.1122] [SPIRES].

[31] D. Chang, W.-F. Chang, C.-H. Chou and W.-Y. Keung, *Large two-loop contributions to* $g-2$ *from a generic pseudoscalar boson*, *Phys. Rev.* **D 63** (2001) 091301 [hep-ph/0009292] [SPIRES];
K.-m. Cheung, C.-H. Chou and O.C.W. Kong, *Muon anomalous magnetic moment, two-Higgs-doublet model and supersymmetry*, *Phys. Rev.* **D 64** (2001) 111301 [hep-ph/0103183] [SPIRES];
A. Arhrib and S. Baek, *Two-loop Barr-Zee type contributions to* $(g-2)_\mu$ *in the MSSM*, *Phys. Rev.* **D 65** (2002) 075002 [hep-ph/0104225] [SPIRES];
C.-H. Chen and C.Q. Geng, *The muon anomalous magnetic moment from a generic charged Higgs with SUSY*, *Phys. Lett.* **B 511** (2001) 77 [hep-ph/0104151] [SPIRES].

[32] For a recent review, see, for example, D. Stöckinger, *The muon magnetic moment and supersymmetry*, *J. Phys.* **G 34** (2007) R45 [hep-ph/0609168] [SPIRES].

[33] M. Pospelov and A. Ritz, *Electric dipole moments as probes of new physics*, *Annals Phys.* **318** (2005) 119 [hep-ph/0504231] [SPIRES].

[34] M.J. Ramsey-Musolf and S. Su, *Low energy precision test of supersymmetry*, *Phys. Rept.* **456** (2008) 1 [hep-ph/0612057] [SPIRES].

[35] T. Ibrahim and P. Nath, *CP violation from standard model to strings*, *Rev. Mod. Phys.* **80** (2008) 577 [arXiv:0705.2008] [SPIRES].

JHEP06(2009)020

[36] J.R. Ellis, J.S. Lee and A. Pilaftsis, *Electric dipole moments in the MSSM reloaded*, *JHEP* **10** (2008) 049 [arXiv:0808.1819] [SPIRES].

[37] Muon (g-2) collaboration, G.W. Bennett et al., *An improved limit on the muon electric dipole moment*, arXiv:0811.1207 [SPIRES].

[38] B.C. Regan, E.D. Commins, C.J. Schmidt and D. DeMille, *New limit on the electron electric dipole moment*, *Phys. Rev. Lett.* **88** (2002) 071805 [SPIRES].

[39] C.A. Baker et al., *An improved experimental limit on the electric dipole moment of the neutron*, *Phys. Rev. Lett.* **97** (2006) 131801 [hep-ex/0602020] [SPIRES].

[40] M.V. Romalis, W.C. Griffith and E.N. Fortson, *A new limit on the permanent electric dipole moment of* $^{199}$Hg, *Phys. Rev. Lett.* **86** (2001) 2505 [hep-ex/0012001] [SPIRES].

[41] Y.K. Semertzidis et al., *Sensitive search for a permanent muon electric dipole moment*, hep-ph/0012087 [SPIRES].

[42] T. Ibrahim, U. Chattopadhyay and P. Nath, *Constraints on explicit CP-violation from the Brookhaven muon* $g-2$ *experiment*, *Phys. Rev.* **D 64** (2001) 016010 [hep-ph/0102324] [SPIRES].

[43] J.S. Lee et al., *CPsuperH: a computational tool for Higgs phenomenology in the minimal supersymmetric standard model with explicit CP-violation*, *Comput. Phys. Commun.* **156** (2004) 283 [hep-ph/0307377] [SPIRES];
J.S. Lee, M. Carena, J. Ellis, A. Pilaftsis and C.E.M. Wagner, *CPsuperH2.0: an improved computational tool for Higgs phenomenology in the MSSM with explicit CP-violation*, *Comput. Phys. Commun.* **180** (2009) 312 [arXiv:0712.2360] [SPIRES].

[44] J. Guasch, W. Hollik and S. Penaranda, *Distinguishing Higgs models in* $H \to b\bar{b}/H \to \tau^+\tau^-$, *Phys. Lett.* **B 515** (2001) 367 [hep-ph/0106027] [SPIRES].

[45] M.S. Carena, S. Mrenna and C.E.M. Wagner, *MSSM Higgs boson phenomenology at the Tevatron collider*, *Phys. Rev.* **D 60** (1999) 075010 [hep-ph/9808312] [SPIRES].

[46] T. Ibrahim and P. Nath, *Weak isospin violations in charged and neutral Higgs couplings from SUSY loop corrections*, *Phys. Rev.* **D 69** (2004) 075001 [hep-ph/0311242] [SPIRES].

[47] J.R. Ellis, J.S. Lee and A. Pilaftsis, *LHC signatures of resonant CP-violation in a minimal supersymmetric Higgs sector*, *Phys. Rev.* **D 70** (2004) 075010 [hep-ph/0404167] [SPIRES].

[48] M.S. Carena, J.R. Ellis, A. Pilaftsis and C.E.M. Wagner, *CP-violating MSSM Higgs bosons in the light of LEP 2*, *Phys. Lett.* **B 495** (2000) 155 [hep-ph/0009212] [SPIRES].

[49] ALEPH collaboration, S. Schael et al., *Search for neutral MSSM Higgs bosons at LEP*, *Eur. Phys. J.* **C 47** (2006) 547 [hep-ex/0602042] [SPIRES].

[50] P. Franzini et al., *Limits on Higgs bosons, scalar-quarkonia, and* $\eta_b$*'s from radiative upsilon decays*, *Phys. Rev.* **D 35** (1987) 2883 [SPIRES];
J.S. Lee and S. Scopel, *Lightest Higgs boson and relic neutralino in the MSSM with CP-violation*, *Phys. Rev.* **D 75** (2007) 075001 [hep-ph/0701221] [SPIRES].

[51] See, for example, A. Pilaftsis and C.E.M. Wagner, *Higgs bosons in the minimal supersymmetric standard model with explicit CP-violation*, *Nucl. Phys.* **B 553** (1999) 3 [hep-ph/9902371] [SPIRES].

JHEP06(2009)020